

# Width distribution of contact lines on a disordered substrate

Sébastien Moulinet<sup>1\*</sup>, Alberto Rosso<sup>2</sup>, Werner Krauth<sup>1</sup>, Etienne Rolley<sup>1</sup>

<sup>1</sup>*CNRS-Laboratoire de Physique Statistique de l'École Normale Supérieure, 24 rue Lhomond, 75231 Paris, France*

<sup>2</sup>*Université de Genève, DPMC, 24 Quai Ernest Ansermet, CH-1211 Genève 4, Switzerland*

(Dated: October 8, 2003)

We have studied the roughness of a contact line of a liquid meniscus on a disordered substrate by measuring its width distribution. The comparison between the measured width distribution and the width distribution calculated in previous works, extended here to the case of open boundary conditions, confirms that the Joanny-de Gennes model is not sufficient to describe the dynamics of contact lines at the depinning threshold. This conclusion is in agreement with recent measurements which determine the roughness exponent by extrapolation to large system sizes.

PACS numbers: 46.65.+g,64.60.Ht,68.45.Gd

The physics of elastic interfaces in random media is involved in a vast class of problems, such as domain walls in ferromagnetic [1] or ferroelectric [2] systems, and propagation of cracks in solids [3]. A notorious example of an elastic interface is provided by the contact line of a liquid meniscus on a disordered substrate [4, 5, 6, 7].

In the past years, much effort has been devoted to shed light on both the equilibrium properties and the dynamics of this system [8, 9, 10], which is characterized by long-range interactions. Very recently, experiments with water or Helium moving on a substrate characterized by a well controlled disorder [10, 11], have explored the depinning threshold. In this regime [12, 13] the contact line, driven by an external force, moves very slowly. The study of the roughness of the interface, and in particular its scaling behavior, turns out to be a fundamental tool to test our understanding of the physics of systems in which the elasticity and the disorder compete in determining the shape of the interface.

In Fig. 1 we display an experimental sample: a glass plate with Chromium impurities (clear dots), partially covered by a water meniscus (dark region). The so-called contact line is separating the wet and dry regions. The contact line is defined by an internal coordinate  $x$  and by the height  $h$  along the motion direction. We observe that a single-valued height function  $h(x)$  is sufficient to characterize the shape of the contact line. A sample of size  $L = 500 \mu\text{m}$  extracted from the image is also shown in Fig. 1; to analyze its geometric properties we are interested in the deviations from the mean height  $u(x) = h(x) - \langle h \rangle$ , with  $\langle \dots \rangle = 1/L \int_0^L dx \dots$ . The mean square width is defined as  $w^2 = \langle u^2(x) \rangle$ . The roughness exponent  $\zeta$  is introduced by considering an ensemble of lines of size  $L$ , where  $L$  must be larger than the lengths which characterize the disorder. Averaging over this ensemble, we obtain  $\overline{w^2} \propto L^{2\zeta}$  [12].

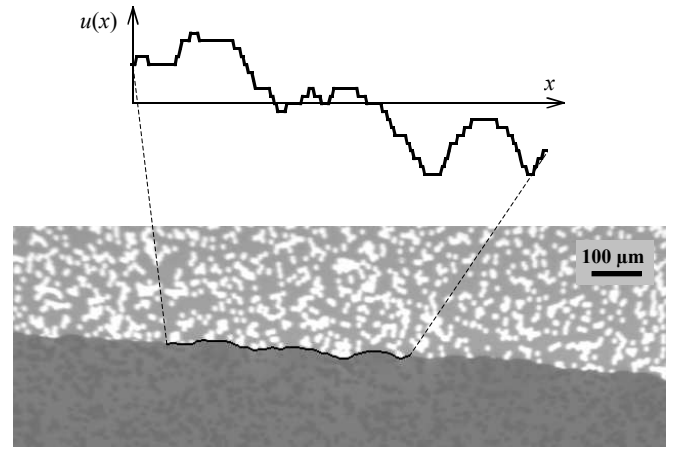


FIG. 1: Bottom: image of a water meniscus receding on a disordered substrate. The wet region is darker. Chromium defects appear as clear dots on the dry region. Top: sample of size  $L = 500 \mu\text{m}$  extracted from the digitalized contact line.  $u(x)$  is the deviation from the mean height averaged over the sample.

The theoretical evaluation of the exponent  $\zeta$  has been up to now based on the assumption that the motion of the line at the threshold is quasi-static [13]; this assumption was shown to be valid for most viscous fluids [11]. This means that the equation of motion of the height  $h(x)$  can be derived from an energy function, which incorporates the potential energy due to the driving force  $f$  and the disorder potential  $\eta(x, h)$ , as well as an elastic energy. According to this hypothesis, the equation of motion for  $h(x)$  at zero temperature is:

$$\frac{\partial}{\partial t} h(x) = f + \eta(x, h) - k \int dx_1 \frac{h(x) - h(x_1)}{(x - x_1)^2}. \quad (1)$$

The last term in Eq. 1 accounts for the long-range elastic force calculated by Joanny and de Gennes [4]. At the equilibrium, independent approaches within Eq. 1 led consistently to the value  $\zeta = 1/3$  [7, 8, 14]. At the depinning threshold, the determination of the roughness exponent stimulated a large debate [7, 13, 15, 16]: finally,

\*now at LPMCN, Université Claude Bernard, 43 Boulevard du 11 novembre 1918, 69622 Villeurbanne Cedex, France

extended renormalization group calculations up to the two-loop order proved that  $\zeta$  is larger than  $1/3$  [17]. This finding was confirmed by a numerical study by means of an exact algorithm, which is able to detect directly the blocked interface at the depinning threshold: the precise resulting value is  $\zeta = 0.388 \pm 0.002$  [18].

In spite of the large amount of theoretical work devoted to the subject, experiments are very few (see [19] and references therein). The main difficulty consists in controlling the disorder; in Ref. [11] this difficulty has been overcome by using photolithographic techniques. Small squares of Chromium (size:  $10 \times 10 \mu\text{m}^2$ ) were deposited randomly on a glass plate, such that the 22% of the surface is covered. This procedure generates a disorder correlated on a scale  $\xi \sim 10 \mu\text{m}$ , sufficiently large to prevent thermal fluctuations from playing any role. The correlation length  $\xi$  is more than two orders of magnitude below the capillary length  $L_c$  ( $\sim 2.5\text{mm}$  in this system) where gravity begins to limit the fluctuations. When the experiment is carried out, the glass plate is withdrawn very slowly from the liquid bath at a fixed velocity ranging between 0.2 and  $20 \mu\text{m/s}$ . The liquid is pure water or an aqueous solution of glycerol with a viscosity up to 20 times that of water. One observes that the shape of the contact line is independent of the velocity. This is a clear signature of the depinning limit [11]. From these measurements it has been obtained, for  $2\xi \leq L \leq L_c/2$ ,  $\zeta = 0.51 \pm 0.03$ , in disagreement with all theoretical predictions [18].

The discrepancy between the theoretical and the measured roughness exponent suggest that a richer model, more complicated than the one described by Eq. 1, is needed to account for the critical behavior of the contact line at the depinning. However, as the range of accessible scales is less than two orders of magnitude, the rigorous determination of the exponent  $\zeta$  is a very delicate experimental task. Thus, to reach more convincing conclusions, it is desirable to compare some other universal quantities characterizing the depinning threshold. In particular, special care must be devoted to evaluate finite size effects, which could affect drastically the final results. To this purpose, we study here the complete width distribution  $P(w^2)$ , and we compare our theoretical predictions, based on the solution of Eq. 1, to experimental data.

The theoretical studies performed on systems without disorder such as stochastic models [20, 21, 22] or magnetic systems [23] have shown that it is possible to express  $P(w^2)$  in a universal scaling form:

$$P(w^2) = \frac{1}{w^2} \phi(x = w^2/\bar{w}^2), \quad (2)$$

where  $x$  is the renormalized width  $w^2/\bar{w}^2$ . In Eq. 2 the size dependence appears only through the average  $\bar{w}^2$ : the non-trivial scaling function  $\phi(x)$  is universal and characterizes a full class of systems. Recently [24], the

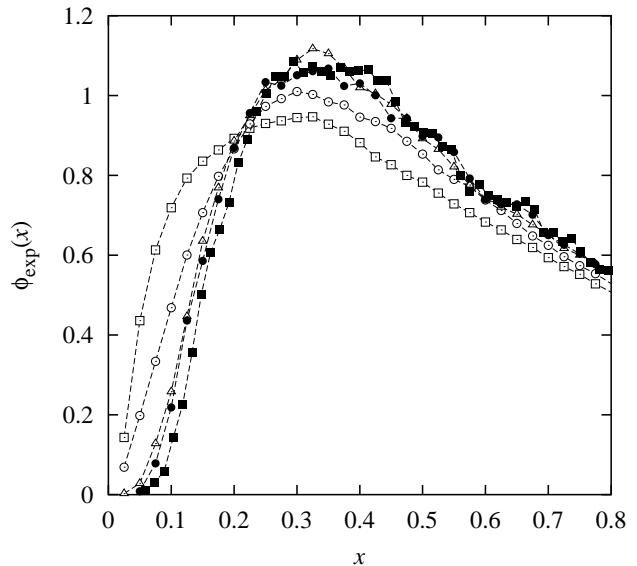


FIG. 2: Experimental scaling function  $\phi_{\text{exp}}(x)$ : study of finite size effects. Open symbols: Aqueous solution of glycerol,  $v = 1 \mu\text{m/s}$  (square:  $L = 124 \mu\text{m}$ , circle:  $L = 186 \mu\text{m}$ , triangle:  $L = 372 \mu\text{m}$ ). Full symbols: water (circle:  $L = 366 \mu\text{m}$ ,  $v = 20 \mu\text{m/s}$ , square:  $L = 500 \mu\text{m}$ ,  $v = 1 \mu\text{m/s}$ ). We observe that for  $L > 300 \mu\text{m}$  the finite size effects are negligible and the scatter of the data is mostly due to the finite width of histogram bins. In this way we have access to the large scale form of  $\phi_{\text{exp}}(x)$ .

same scaling properties have been proved for elastic interfaces in random media at the depinning threshold. The width distribution of these systems is, for all intents and purposes, given by a generalized Gaussian approximation of independent modes, which decay with a characteristic propagator  $G(q) \sim q^{d+2\zeta}$ . Within this approximation, for interfaces of a fixed internal dimension and for the required boundary conditions,  $\phi(x)$  depends only on the roughness exponent  $\zeta$ .

In order to determine the experimental width distribution we have employed the same experimental setup as described in Ref. [11]; the contact line is imaged with a progressive scan CCD camera equipped with a microscope. Two different magnifications are used, corresponding to a pixel of size  $\Delta x = 6.10$  and  $\Delta x = 2.14 \mu\text{m}$ . After the analysis of the images we obtain a digitized line of 760 pixels. Thanks to the good contrast and signal-to-noise ratio of the CCD, the final resolution is still one pixel. The experimental lines are cut into samples of size  $L = n\Delta x$ , where  $n$  is the number of pixels in the sample. From each line we extract an ensemble of  $(760 - n)$  samples, whose width is simply given by  $w^2 = 1/L \sum_{i=1}^n u_i^2$ . These operations are repeated over all the configurations detected by the camera. Clearly the values of  $w^2$  are not independent [31], but this procedure ensures that no information is lost.

The histogram derived by the data gives access to the

universal function  $\phi_{\text{exp}}(x)$  which is plotted in Fig. 2 for various sizes  $L$  and for various experimental conditions. For samples of size in the range  $300 \mu\text{m} < L < 800 \mu\text{m}$ , the obtained function  $\phi_{\text{exp}}(x)$  is independent of the size, the viscosity and the velocity of the receding meniscus. In smaller samples ( $100 \mu\text{m} < L < 300 \mu\text{m}$ ), the distribution is sensitive to finite size effect related to the details of the way the disorder is created. Samples bigger than  $L = 800 \mu\text{m}$  cannot be treated due to the significant statistical noise.

At this stage, the universal function  $\phi(x)$  which we have extracted from experiments can be compared to the theoretical evaluation within the Gaussian approximation. Previous theoretical works [20, 21, 22, 24] deal with samples where the boundary conditions were periodic, which is obviously not the case of our experiment (see Fig. 1). In order to calculate  $\phi(x)$  in the Gaussian approximation for open boundary conditions, we generalize the discussion of Ref. [24]. The main difference, as it is briefly discussed in Refs. [25, 26], lays in the Fourier decomposition of the path  $u(x)$ . In the case of open boundary conditions, the general path of size  $L$  takes the form:

$$u(x) = \sum_{n=1}^{\infty} a_n \cos(\tilde{q}_n x), \quad (3)$$

where  $\tilde{q}_n = \frac{\pi n}{L}$ . The probability associated with this path is:

$$\mathcal{P}[u] = \mathcal{N} \prod_{n=1}^{\infty} e^{-1/2 a_n^2 G_n^{-1}}, \quad (4)$$

where  $\mathcal{N}$  is the normalization factor and, for large  $L$ , the exact disorder-averaged 2-point function  $G_n$  takes the form  $G_n \rightarrow C/n^{1+2\zeta}$ . The expression for  $P(w^2)$  follows from the generating functions of the moments:

$$W(z) = \int_0^{\infty} dw^2 P(w^2) e^{-zw^2}. \quad (5)$$

Similarly to the case of periodic boundary conditions [24], we write

$$W(z) = \prod_n \left( \frac{1}{G_n^{-1} z + 1} \right)^{1/2}$$

The function  $\phi(x)$  is given by  $W(z)$  through an inverse-Laplace transform:

$$\phi(x) = \int_{-i\infty}^{+i\infty} \frac{dz}{2\pi i} e^{zx} \prod_{n=1}^{\infty} \left( \frac{n^\alpha A}{z + n^\alpha A} \right)^{1/2}, \quad (6)$$

with  $A = \frac{1}{2} \sum_{n=1}^{\infty} \frac{1}{n^\alpha}$  and  $\alpha = 1 + 2\zeta$ . This complex integral can be written as a sum of all the tadpole contributions:

$$\phi(x) = \sum_{n=0}^{\infty} \frac{(-1)^n}{\pi} \int_{a_1(n)}^{a_2(n)} dz e^{zx} \prod_{m=1}^{\infty} \left| \frac{m^\alpha A}{z + m^\alpha A} \right|^{1/2}, \quad (7)$$

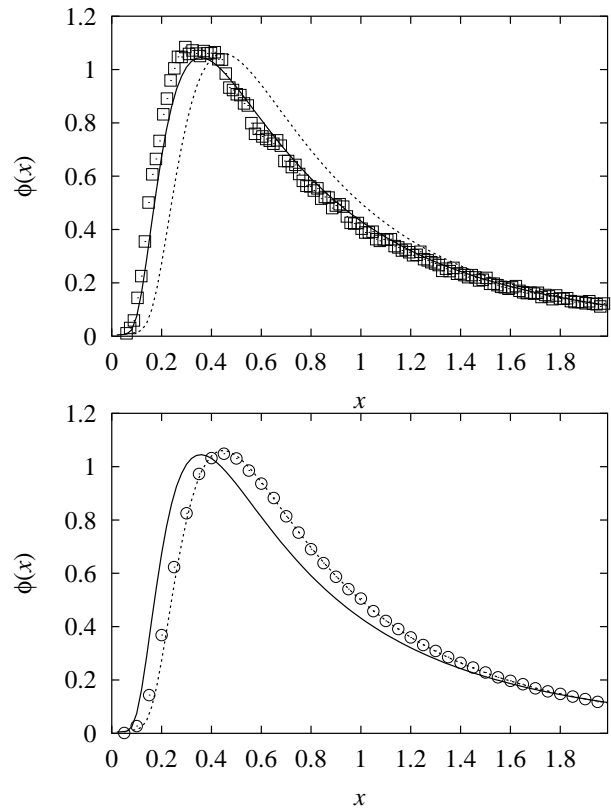


FIG. 3: Top: we compare the scaling function  $\phi_{\text{exp}}(x)$  obtained from the experimental data (squares: water  $L = 500 \mu\text{m}$ ,  $v = 1 \mu\text{m/s}$ ) with the curves calculated by means of Eq. 7. We notice the good agreement with the curve obtained for  $\zeta = 0.505$  (continuum line). Bottom: we compare the scaling function  $\phi_{\text{num}}(x)$  obtained from the numerical data (circles:  $L = 32$ ,  $10^6$  independent samples) with the curves calculated by means of Eq. 7. We notice a perfect agreement with the curve obtained for  $\zeta = 0.39$  (dashed line).

with  $a_1 = -A(2n+2)^\alpha$  and  $a_2 = -A(2n+1)^\alpha$ . The product in Eq. 7 converges slowly, and several thousand terms need to be computed. Once this is done, however, only a few terms in the external sum of Eq. 7 are sufficient to obtain  $\phi(x)$  with high precision.

In Ref. [24] it is discussed how the width distribution of an interface moving in a random medium, characterized by short range elastic interactions, is described in an excellent way by the distribution obtained within the Gaussian approximation. For sake of completeness, we show the scaling function  $\phi_{\text{num}}(x)$  computed from the numerical study of Eq. 1 at the depinning threshold. We use the algorithm from Ref. [18] and we calculate critical lines of size  $L = 256$  with periodic boundary conditions.  $\phi_{\text{num}}(x)$  is obtained with the same procedure employed to deal with experimental data, by using samples of size  $L = 32$ . In this way, we find the scaling function corresponding to the case of open boundary conditions.

In Fig. 3 we summarize our results. As expected from Ref. [24], the function  $\phi_{\text{num}}$  derived from the numerical

study of Eq. 1 is in perfect agreement with the function obtained in the Gaussian approximation with  $\zeta = 0.39$ . The shape of  $\phi_{\text{exp}}$  is also in good agreement with the calculated function, but it is clearly shifted with respect to  $\phi_{\text{num}}$  and best approximated with  $\zeta = 0.505$ .

To our knowledge, this kind of analysis is applied for the first time to experimental data. It offers the possibility to evaluate the roughness exponent from a unique value of  $L$  and it can be useful if the accessible range of scaling is small. Moreover we have detected finite size effects that are invisible on the simple representation of  $\overline{w^2}(L)$ . Due to the reduction of range of scaling, the analysis of  $\overline{w^2}(L)$  yields  $\zeta = 0.52 \pm 0.04$ , slightly larger than the previous determination [11].

Our study confirms that a real contact line cannot be described by the Joanny-de Gennes model. The same type of equation of motion has been proposed to describe the propagation of crack fronts [3]. In this case the experiments yield  $\zeta \sim 0.5 - 0.6$  [27, 28]. Dynamical mechanism have been introduced recently [29] to account for the anomalous value of  $\zeta$  for crack fronts. On the other hand, for the contact line, a precise analysis of the motion justifies the quasi-static hypothesis [11] and no such dynamical mechanism has to be considered. The study of the width distribution of crack fronts could help to understand if the two systems belong to the same universality class and to unravel the origin of the discrepancy between the theoretical and the experimental values of  $\zeta$ . In fact, in both cases, the derivation of the long-range elastic term in Eq. 1 is obtained by a development to first order in the deformation. This truncation avoids the existence in the equation of motion of non-harmonic corrections which, as it has been shown for the short-range elastic interactions [30], can drastically change the critical behavior of the interface. Moreover the presence of non-linear terms has already been introduced in Ref. [9] to understand the dynamics of a contact line in the high velocity limit. It would be very interesting to study the effect of these terms on the critical properties at the depinning transition. Unfortunately, up to now the numerical computation of this new equation of motion is impossible because of the presence of non-convex terms in the elastic energy.

We thank C. Guthmann, P. Le Doussal, J. Vannimenus and J. K. Wiese for useful discussions.

- 
- [1] S. Lemerle, J. Ferré, C. Chappert, V. Mathet, T. Giamarchi, and P. Le Doussal, Phys. Rev. Lett. **80**, 849 (1998).  
 [2] T. Tybell, P. Paruch, T. Giamarchi, and J. M. Triscone, Phys. Rev. Lett. **89**, 097601 (2002).  
 [3] H. Gao and J. R. Rice, J. Appl. Mech. **56**, 828 (1989).

- [4] J. Joanny and P. de Gennes, J. Chem. Phys. **81**, 552 (1984).  
 [5] Y. Pomeau and J. Vannimenus, J. Colloid Int. Science **104**, 477 (1985).  
 [6] J. Joanny and M. Robbins, J. Chem. Phys. **92**, 3206 (1990).  
 [7] D. Ertaş and M. Kardar, Phys. Rev. E **49**, R2532 (1996).  
 [8] A. Hazareezing and M. Mézard, Phys. Rev. E **60**, 1269 (1999).  
 [9] R. Golestanian and E. Raphaël, Europhys. Lett. **55**, 228 (2001).  
 [10] A. Prevost, E. Rolley, and C. Guthmann, Phys. Rev. B **65**, 064517 (2002).  
 [11] S. Moulinet, C. Guthmann, and E. Rolley, Eur. Phys. J. E **8**, 437 (2002).  
 [12] T. Nattermann, S. Stepanow, L. H. Tang, and H. Leschhorn, J. Phys. (Paris) **2**, 1483 (1992).  
 [13] O. Narayan and D. Fisher, Phys. Rev. B **48**, 7030 (1993).  
 [14] M. Robbins and J. Joanny, Europhys. Lett. **3**, 729 (1987).  
 [15] A. Tanguy, M. Gounelle, and S. Roux, Phys. Rev. E **58**, 1577 (1998).  
 [16] S. Ramanathan and D. Fisher, Phys. Rev. B **58**, 6026 (1998).  
 [17] P. Chauve, P. Le Doussal, and K. Wiese, Phys. Rev. Lett. **86**, 1785 (2001).  
 [18] A. Rosso and W. Krauth, Phys. Rev. E **65**, R025101 (2002).  
 [19] R. Johnson and R. Dettre, in *Wettability*, edited by J. C. Berg (Marcel Dekker, New York, 1993).  
 [20] G. Foltin, K. Oerding, Z. Rácz, R. Workman, and R. Zia, Phys. Rev. E **50**, R639 (1994).  
 [21] M. Plischke, Z. Rácz, and R. Zia, Phys. Rev. E **50**, 3589 (1994).  
 [22] Z. Rácz and M. Plischke, Phys. Rev. E **50**, 3530 (1994).  
 [23] S. T. Bramwell and *et al.*, Phys. Rev. Lett. **84**, 3744 (2000).  
 [24] A. Rosso, W. Krauth, P. Le Doussal, J. Vannimenus, and K. Wiese (2003).  
 [25] T. Antal, M. Droz, G. Györgyi, and Z. Rácz, Phys. Rev. E **65**, 046140 (2001).  
 [26] P. Le Doussal and K. Wiese (2003), cond-mat/0301465.  
 [27] J. Schmittbuhl and K. J. Måløy, Phys. Rev. Lett. **78**, 3888 (1997).  
 [28] A. Deleplace, J. Schmittbuhl, and K. J. Måløy, Phys. Rev. E **60**, 1337 (1999).  
 [29] E. Bouchaud, J. P. Bouchaud, D. S. Fisher, S. Ramanathan, and J. R. Rice, J. Mech. Phys. Solids **50**, 1703 (2002).  
 [30] A. Rosso and W. Krauth, Phys. Rev. Lett. **87**, 187002 (2001).  
 [31] Let us evaluate the number of independent configurations that can be obtained in our experiment. Using, for example, the lower magnification the observed length of the line is 4.7 mm. During an experiment the total displacement is of the order of 15 mm. As the maximum width of the contact line is  $\sim 30 \mu\text{m}$ , the number of independent configuration is 500. As an example, for a size  $L = 500 \mu\text{m}$ ,  $\phi$  is then determined from typically 5000 independent samples.